COMPUTER SIMULATION OF BEAMS IN HIGH ENERGY ELECTRON STORAGE RINGS*

R. H. Siemann
Laboratory of Nuclear Studies, Cornell University, Ithaca, New York 14853

Summary

Computer simulation studies of single beam stability have been able to reproduce observed phenomena in PEP and PETRA. These studies use wakefields calculated from RF cavity dimensions and Monte Carlo techniques to study the effects of these wakefields. In this paper the procedures used are reviewed, and some results are presented.

Introduction

Experiences at PETRA[1,2] and PEP[3] have shown the importance of single beam stability questions in determining the performance of large e^+e^- storage rings. In particular, the need to study these questions during the design phase of proposed rings has become clear. Such a study requires knowledge of accelerator wakefields and the inclusion of these wakefields in the equations of motion for beam particles. Computer programs[4-10] which calculate the needed wakefields are now available, and several Monte Carlo studies[11,12] of single beam stability are in progress or completed. The computer simulation work has concentrated on PEP and PETRA to allow the comparison of results with experimental observations, and the agreement with experiment is reasonable.

This paper will review the techniques for calculating wakefields and studying beam dynamics in the presence of wakefields.

Wakefield Calculations

The available computer programs to calculate wakefields have been written for the case of rotationally symmetric structures. In the case of large electron storage rings the dominant contribution to the impedance is from the RF cavities, and it is reasonable to approximate these cavities as rotationally symmetric.

For cavities of rotational symmetry and particles traveling at the speed of light the voltage a particle experiences when following a distance ct behind a unit-charge, δ-function particle is[13]:

$$V_\delta(r,\Delta,\phi,t) = \int_{-\infty}^{\infty} dz \int_{-\infty}^{\infty} dt'\ E_z(r,\Delta,\phi,t',z)\ \delta(t'-(t+z/c)) \qquad (1)$$

$$= \sum_{k=0}^{\infty} \Delta^k\, r^k \cos k\phi\ V_k(t)\ .$$

The quantities Δ, r and φ are defined in figure 1. In this equation E_z is the field excited by the unit-charge particle. The transverse impact is

$$\Delta \vec{P}_\perp(r,\Delta,\phi,t) = \frac{q}{c} \int_{-\infty}^{\infty} dz \int_{-\infty}^{\infty} dt'\ (\vec{E}+c\hat{z}\times\vec{B})_\perp\, \delta(t'-(t+z/c)) \qquad (2)$$

$$= \frac{q}{c} \sum_{k=1}^{\infty} k\, \Delta^k\, r^{k-1}\, W_k(t)\ (\hat{r}\cos k\phi - \hat{\phi}\sin k\phi).$$

The functions $W_k(t)$ and $V_k(t)$ are related by[15]

$$W_k(t) = -c\int_{-\infty}^{t} dt'\ V_k(t')\ . \qquad (3)$$

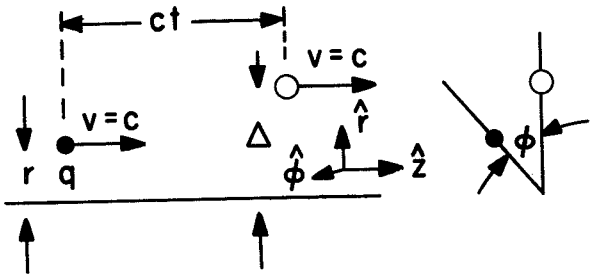

Fig. 1. A unit-charge, δ-function particle a distance Δ from the symmetry axis of a rotationally symmetric structure is followed at a distance ct by a particle of charge q a distance r from the axis. φ is the azimuthal angle between the particles.

For the mode number k=0 the voltage V_δ, is independent of r, Δ, and φ; in addition k=0 does not produce any transverse deflection. For k=1 V_δ is linear in r and Δ, and there is a transverse impact. The impact is independent of r and φ ($(\hat{r}\cos\phi - \hat{\phi}\sin\phi)$ points in a direction independent of φ) and is linear in Δ, the displacement of the source particle. Computer simulations to date have been limited to k=0,1.

Two general approaches have been used to calculate the time dependent terms in eqs. 1 and 2. The first of these approaches, time domain integration, uses difference equations to approximate the differential form of Maxwell's equations[16]. This technique was introduced to accelerator physicists by Weiland[4] who used it to calculate the k=0 wakefield. Since then he has written a program[5] for k=0,1,... , and Aharonian et al.[6] have written one for k=1. In all cases the wakefields cannot be calculated for a δ-function charge exciting the cavity. A smooth charge distribution (typically a Gaussian) must be used, and the frequency content of the wakefield is limited to values below some cutoff. For a Gaussian the angular frequency cutoff is approximately equal to the inverse of the rms bunch length. Figure 2 shows typical wakefields calculated by this technique.

The alternative approach is to find the normal modes of the cavity structure and construct the wakefield by summing over these modes. For example, for k=0[14,17]

$$V_o(t) = -2 \sum_\lambda K_\lambda \cos\omega_\lambda t. \qquad (4)$$

The K_λ's are loss factors for the modes and ω_λ's are the resonant frequencies. For arbitrarily shaped rotationally symmetric cavities SUPERFISH[7] can be used to calculate the K_λ's and ω_λ's for modes with k=0 or URMEL[8] can be used for k=0,1,... . The maximum frequency mode which can be calculated using these programs is typically the cutoff frequency of the beam pipe. Since this frequency is much lower than that needed, approximations are used to extend the frequency range. These approximations use KN7C[9] and TRANSVERSE[10].

KN7C (k=0) and TRANSVERSE (k=1,...) are programs to find the parameters of modes in an infinite, periodic, disk-loaded waveguide; their primary use has been the calculation of the SLC wakefields[14]. In this latter application over 400 modes are identified

*Work supported in part by the National Science Fndtn.

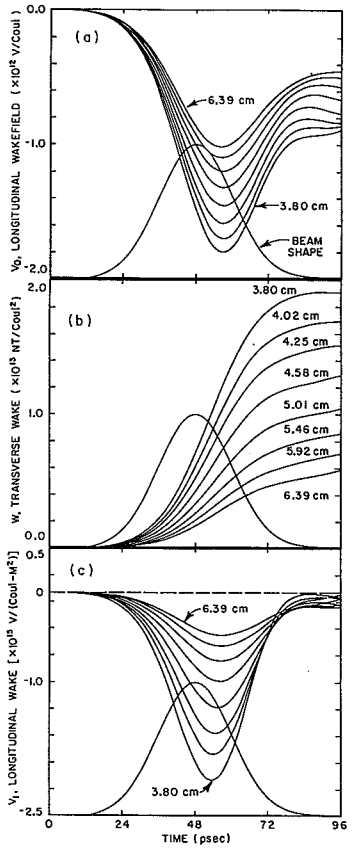

Fig. 2. Wakefields calculated for PEP cavities. The curves are for different beam pipe radii. The longitudinal wakefields for k=0 and k=1 are shown in a) and c). b) shows the k=1 transverse wakefield. These wakefields were calculated using the programs described in refs. 4 and 6.

and summed in eq. 4 (or its higher k equivalent). At very high frequencies even this number of modes is inadequate, and an "optical resonator model"[9,14,18] is used to extend the frequency range. For arbitrarily shaped cavities, KN7C and TRANSVERSE modes are used to extend the frequency range of the wakefield to above the beam pipe cutoff frequency[11,19,20].

Several comparisons have been made between wakefields calculated by time domain integration and those calculated by an analysis of modes[19,21-23]. The agreement is always good.

Modelling of Beam Dynamics

The equations of motion for particles in an accelerator are modified to include wakefields and other coherent effects. In the longitudinal the synchrotron motion, radiation damping, and radiation fluctuations are augmented by Robinson damping[24] and wakefields. The former term leads to the damping of coherent longitudinal dipole oscillations and is due to the interaction of the beam with the fundamental mode of the accelerating cavities. The equations of motion are[25]

$$t_m(n) = t_m(n-1) + \frac{\alpha T_o}{E_o}\,\varepsilon_m(n) \qquad (5a)$$

$$\varepsilon_m(n) = \varepsilon_m(n-1) - \frac{2T_o}{\tau_\varepsilon}\,\varepsilon_m(n-1) - \frac{2T_o}{\tau_D}\,\bar{\varepsilon}\,(n-1)$$

$$-U_o(1 - \cos(\omega_{rf}\, t_m(n-1))) - \hat{U}\sin(\omega_{rf}\, t_m(n-1))\sin\phi_s$$

$$+ 2\sigma_{\varepsilon o}\sqrt{\frac{T_o}{\tau_\varepsilon}}\,p_m(n) + V_m^L(n)\ . \qquad (5b)$$

where the symbols are defined on Table I. In these equations m=1,..., M represents the beam particle number, and the argument n specifies the revolution number. The wakefield is the last term in the second equation, and it is dependent on the transverse displacement of particle m and those that precede it in the bunch if the k=1 contribution is included (see eq. 1). This transverse displacement dependence has the potential of driving synchro-betatron resonances[26] which have been observed in one simulation[12].

The approximation which is being made in eq. 5 is that one turn is a sufficiently small fraction of a synchrotron oscillation period that all of the contributions to the wakefield can be combined into a single term. If this is not a good approximation fractions of a turn may have to be considered. Alternatively, it may be possible to combine several turns for very low synchrotron tunes.

In the transverse, wakefields are added to the betatron motion and synchrotron radiation effects

$$z_m(n) = (M_{11}(\varepsilon_m(n))z_m(n-1) + M_{12}(\varepsilon_m(n))z'_m(n-1))\left(1 - \frac{T_o}{\tau_z}\right) + \sqrt{\frac{2E_z\beta_z T_o}{\tau_z}}\,R_m(n)$$

and

$$z'_m(n) = (M_{21}(\varepsilon_m(n))\ z_m(n-1) + M_{22}(\varepsilon_m(n))z'_m(n-1))\left(1 - \frac{T_o}{\tau_z}\right) + \sqrt{\frac{2E_z\,T_o}{\beta_z\,\tau_z}}\,S_m(n) + \frac{W_m^z(n)}{E_o} \qquad (6)$$

The symbols are also defined in Table I. The transfer matrix elements M are made momentum dependent by including chromaticity. The wakefield term gives the angular kick that particle m receives, as eq. 2 shows it depends on the transverse coordinates of particles which precede m but not on the transverse coordinates of m.

In computer simulations one approximates the beam with a number of test particles, M, which is smaller than the actual number of particles on the beam by factors $\sim 10^8$. This has consequences for the treatment of wakefields in eqs. 5 and 6. One approach which has been used extensively[11,20,25,27] is to treat each test particle as a δ-function source and calculate the resultant effect on the other test particles. In the longitudinal this procedure is sensitive to the number of test particles. For example, the energy spread from one simulation[20] is well described as a constant plus a term proportional to $M^{-\frac{1}{2}}$; the result for the energy spread is obtained by extrapolation to $M=\infty$. A second disadvantage of this approach is that

knowledge of the short time (high frequency) wakefields is required.

An alternative is to describe the bunch as a smooth charge distribution, $\rho(t)$, which has sufficient freedom to distort and develop coherent modes[12]. The test particles are used to determine the parameters of $\rho(t)$, and the wakefields needed in eq. 5 and 6 can be obtained from these parameters. The results of this method are insensitive to the number of test particles and (within reasonably unrestrictive bounds) the choice of the form for $\rho(t)$[12]. An additional advantage is the frequency cutoff of $\rho(t)$ gives a maximum frequency needed in the wakefield.

Results

At PEP with certain beam optics the beam current has been limited by a transverse instability which is present at zero chromaticity[3]. Equations 5 and 6 and the wakefields shown in figure 2 have been used to study the instability[12]. Figure 3 is typical of the computer simulation results near the instability threshold. Growth is seen in both the beam size and the mean transverse coordinate. The zero chromaticity instability has been explained by Kohaupt[2] as a mixing between coherent modes of the beam. The Q_S, E_o and β dependences of the threshold current as determined by the simulation are in agreement with those expected by Kohaupt. In addition mixing between two coherent modes is clearly seen in a plot of tunes vs. current (Figure 4).

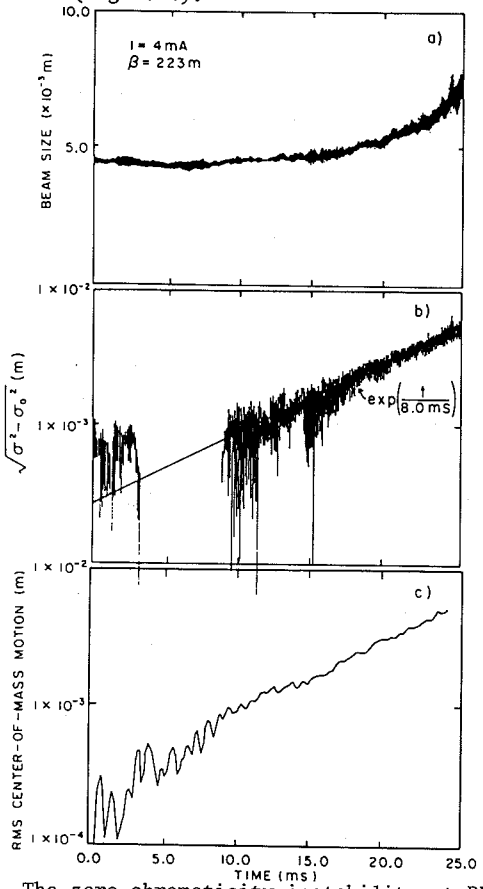

Fig. 3. The zero chromaticity instability at PEP. a) shows the beam size, and b) shows the beam size with the natural beam size subtracted. c) shows that the instability is also seen in the center-of-mass motion.

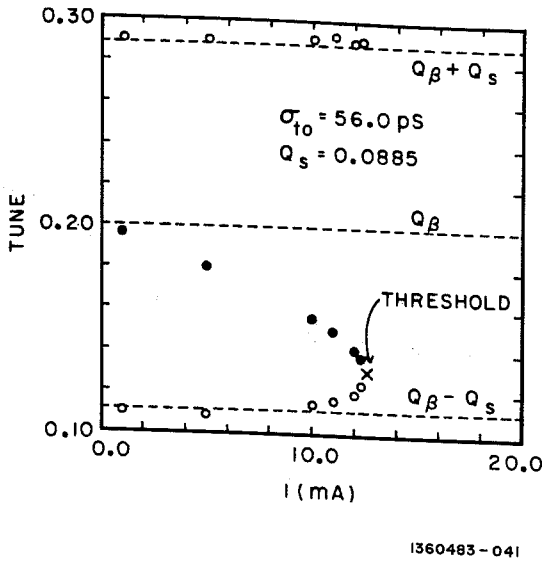

Fig. 4. Tunes for three coherent modes vs. current.

Quantitative comparisons have been made. Using only the wakefields from the RF cavities the simulation finds threshold currents twice as large as the measured threshold currents. This factor of two is in agreement with estimates of the fraction of the transverse impedance due to the RF cavities[3].

The major experimental difference between the transverse instabilities at PEP and PETRA is the observation of significant center-of-mass motion in the former case but not the latter[1-3]. Two computer simulations[11,12] have studied PETRA, and both of them exhibit instabilities without center-of-mass motion. Figure 5 shows results from one of the simulations.

The difference between PEP and PETRA can be understood qualitatively by comparing the imaginary parts of the transverse impedances of the cavities which are shown in fig. 6. (It is the imaginary part of the transverse impedance which causes the tune of the coherent modes to shift with current[28].) Both impedances cross zero around 2 GHz. The lowest order coherent mode of the beam is a mode which exhibits a large center-of-mass motion and has a zero current tune equal to the betatron tune[28]. This mode has a frequency spectrum which is a Gaussian with a mean value of zero and an rms width of $1/2\pi\sigma$ where σ is the rms bunch length. For such a spectrum in PEP (where the natural bunch length is long) there can be little cancellation between the inductive and capacitive parts of the impedance. The tune of the lowest mode should be strongly current dependent, and it is not surprising to see this mode contribute to the instability.

For PETRA the short natural bunch length can cause significant cancellation between the inductive and capacitive impedances and thereby reduce the tune shift of the lowest mode. The effective impedance of the lowest mode is reduced sufficiently to allow higher order coherent modes to mix first; this will lead to an instability with little center-of-mass motion.

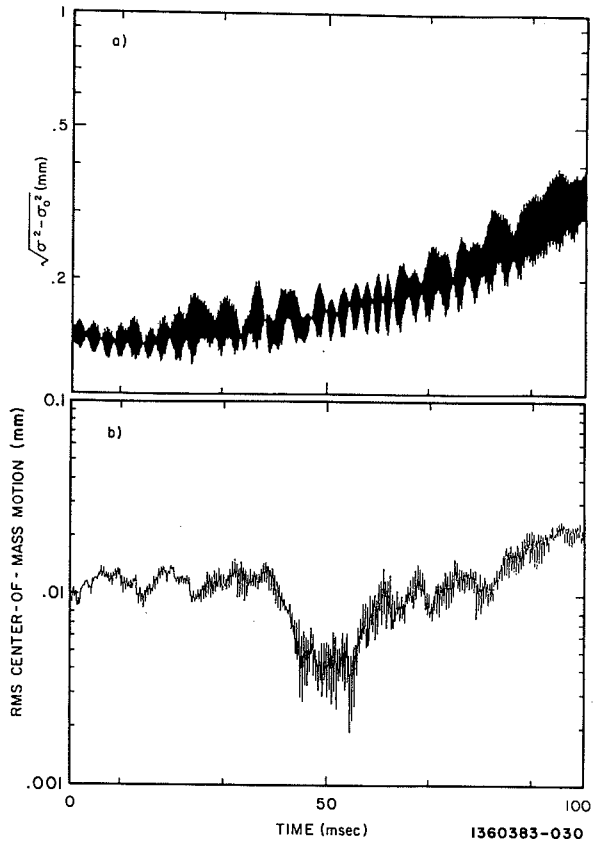

Fig. 5. The zero chromaticity instability in PETRA shows growth in the center-of-mass motion which is much less than the growth in beam size. This is in contrast to the results for PEP shown in figure 3.

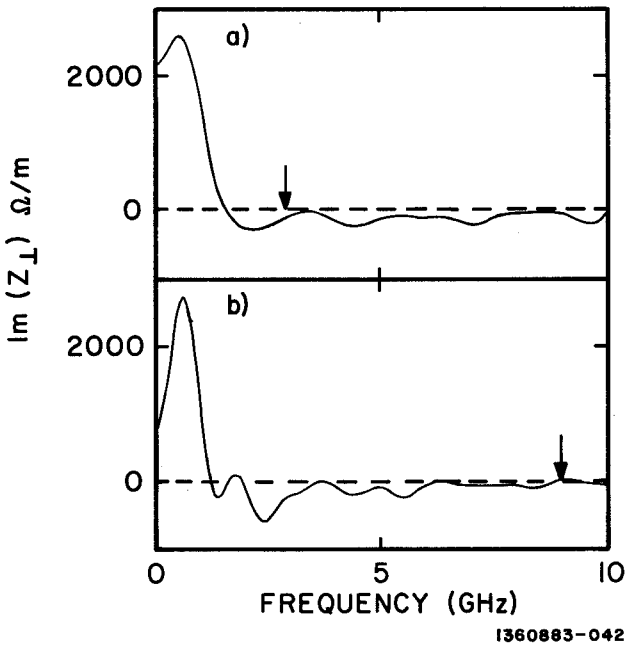

Fig. 6. Imaginary part of the transverse impedance for PEP (a) and PETRA (b). The arrows indicate the rms width of the frequency spectrum of the lowest coherent mode.

Conclusions

The combination of numerical calculations of wakefields and Monte Carlo calculation of beam particle motion has been able to reproduce observed single beam phenomena in PETRA and PEP. This type of analysis should be performed during the design of future accelerators.

References

1. D. Degèle et al., 11th Intnl. Conf. on High Energy Accelerators, CERN, 1980, p.16.
2. R. D. Kohaupt, DESY 80/22, (March 1980).
3. P. B. Wilson and L. Rivkin, PEP-374 (August 1982).
4. T. Weiland, 11th Intnl. Conf. on High Energy Accelerators, CERN, 1980, p.570; T. Weiland CERN, ISR-TH/80-07 (January 1980).
5. T. Weiland, DESY 82/15 (March 1982), NIM to be published.
6. G. Aharonian, R. Meller and R. Siemann, CLNS 82/535 (June 1982), NIM to be published.
7. K. Halbach and R. F. Holsinger, Part. Accel. 7, 213 (1976).
8. T. Weiland, DESY 83/5 (Feb. 1983).
9. E. Keil, NIM 100, 419 (1972).
10. K. Bane and B. Zotter, 11th Intnl. Conf. on High Energy Accelerators, CERN, 1980, p581.
11. D. Brandt, LEP Note 444 (May 1983).
12. R. H. Siemann, IEEE Trans. Nucl. Sci. NS-30, 2373 (1983); R. H. Siemann, CLNS 83/560 (April 1983).
13. This has been shown for k=0 by: R. Sundelin — private comm. (Oct. 1977); A. Piwinski — DESY-M-VM-80-16 (May 1980);
    for infinite repeating structures by: K. Bane and P. B. Wilson, ref. 14; A. Chao, SLAC-PUB-2946 (June 1982);
    and for general rotational symmetry by: R. Siemann, CBN 83-1 (Nov. 1982), T. Weiland, DESY M-83-02 (Feb. 1983).
14. K. Bane, and P. B. Wilson, 11th Intnl. Conf. on High Energy Accelerators, CERN, 1980, p.581.
15. W. K. H. Panofsky and W. A. Wenzel, RSI 27, 967 (1956).
16. Kane S. Yee, IEEE Trans. on Anten. and Propag. AP-14, 302 (1966).
17. K. Bane, CERN/ISR-TH/80-47 (Nov. 1980).
18. D. Brandt and B. Zotter, LEP Note 388 (June 1982).
19. D. Brandt and H. Henke, LEP Note 352 (Feb. 1982).
20. D. Brandt, LEP Note 384 (May 1982).
21. T. Weiland and B. Zotter, Part. Accel. 11 143 (1981).

22. K. Bane and T. Weiland, SLAC/AP-1 (Jan. 1983).

23. D. Brandt, LEP Note 453 (July 1983).

24. K. W. Robinson, CEAL-1010 (Feb. 1964).

25. P. B. Wilson, K. L. F. Bane, and Kohtaro Satoh, IEEE Trans. Nucl. Sci. NS-28, 2525 (1981).

26. R. M. Sundelin, IEEE Trans. Nucl. Sci. NS-26, 3604 (1979).

27. T. Weiland, DESY, 81-088, (Dec. 1981).

28. J. L. Laclare, 11th Intnl. Conf. on High Energy Accelerators, CERN 1980, p.526.

TABLE I: Definition of Symbols used in Equations (5) and (6)

t_m:	deviation from the zero current phase stable time,
ε_m:	deviation from energy equilibrium,
α:	momentum compaction,
T_o:	beam revolution period,
E_o:	beam energy,
τ_ε:	radiation damping time for energy oscillations,
τ_D:	Robinson damping time,
$\bar{\varepsilon}$:	mean energy displacement $(\frac{1}{M}\sum_{m=1}^{M}\varepsilon_m)$,
U_o:	average synchrotron radiation energy loss per turn,
$\hat{U}$:	peak energy gain from rf,
ω_{rf}:	angular frequency of the rf,
ϕ_s:	zero current synchronous phase angle $(= \cos^{-1}(U_o/\hat{U}))$,
$\sigma_{\varepsilon o}$:	natural energy spread of the beam
P_m, R_m, S_m:	Gaussian distributed random numbers with mean = 0 and rms = 1,
V_m^L:	longitudinal wakefield,
x_m, y_m^*:	betatron oscillation coordinates,
x_m', y_m':	slopes of betatron oscillation coordinates,
$M_{11},\ldots,M_{22}$:	the elements of the 2 x 2 transfer matrix (there are separate matrices for horizontal and vertical).
τ_x,τ_y:	radiation damping times for betatron oscillations,
E_x, E_y:	natural emittances of the beam
β_x, β_y:	betatron oscillation amplitude functions at the rf cavities,
W_m^x, W_m^y:	transverse wakefields,

*throughout x denotes horizontal, y denotes vertical, and z is used to denote either.